DOI: 10.19663/j.issn2095-9869.20220228002 http://www.yykxjz.cn/

王新月, 陈生熬, 王程欣, 訾方泽, 常德胜, 许豪, 李大鹏. 叶尔羌高原鳅耳石形态探究及群体判别分析. 渔业科学进展, 2023, 44(4): 201–211
WANG X Y, CHEN S A, WANG C X, ZI F Z, CHANG D S, XU H, LI D P. Otolith morphology and population discrimination of *Triplophysa yarkandensis*. Progress in Fishery Sciences, 2023, 44(4): 201–211

叶尔羌高原鳅耳石形态探究及群体判别分析*

王新月[1] 陈生熬[1,2①] 王程欣[1] 訾方泽[1] 常德胜[1] 许 豪[1] 李大鹏[2]

(1. 塔里木大学生命科学与技术学院 塔里木珍稀鱼类研究中心 新疆 阿拉尔 843300;
2. 华中农业大学水产学院 湖北 武汉 430070)

摘要 为进一步开展叶尔羌高原鳅(*Triplophysa yarkandensis*)不同地理群体分类判别、探明耳石与鱼类生活史的相关机制，本研究基于耳石形态学和鱼类生态学方法，对叶尔羌河、和田河和塔里木河的 734 尾叶尔羌高原鳅耳石与鱼体的形态指标进行了统计分析。结果显示，叶尔羌高原鳅耳石较小，左右微耳石形态无显著差异($P>0.05$)；叶尔羌高原鳅耳石形态指标与体长、体质量呈对数函数关系，R^2 范围在 0.48~0.62；采用鱼体形态学、耳石形态测量法和椭圆傅里叶分析法分别对两两群体进行判别分析，和田河群体与塔里木河群体判别准确率分别为 96.0%、61.4%和 82.2%，叶尔羌河群体与和田河群体判别准确率分别为 93.0%、79.5%和 87.9%，叶尔羌河群体与塔里木河群体判别准确率分别为 96.5%、77.5%和 86.8%。叶尔羌高原鳅耳石形态与鱼体生长的关系极大程度地反映了其个体发育对栖息环境的适应性，且不同地理群体叶尔羌高原鳅耳石形态特征存在显著差异($P<0.05$)。本研究将耳石形态学首次应用于叶尔羌高原鳅种群的鉴别分析，为进一步开展高原鳅属进化分类提供参考，为高原渔业种质资源保护提供了科学依据。

关键词 叶尔羌高原鳅；耳石；形态差异；判别分析

中图分类号 Q954 **文献标识码** A **文章编号** 2095-9869(2023)04-0201-11

叶尔羌高原鳅 *Triplophysa* (*Hedinichthys*) *yarkandensis* (Day, 1877)，隶属鲤形目(Cyprinidformes)、鳅科(Cobitidae)、条鳅亚科(Nemachilinae)、高原鳅属(*Triplophysa*)、鼓鳔鳅亚属(*Hedinichthys*)，是塔里木河水系特有鱼类(郭焱等, 2012)，新疆维吾尔自治区二级重点保护水生动物。目前，其研究主要集中在生长繁殖、养殖及毒性实验、遗传多样性等方面，对其不同地理群体开展分类鉴别仅见鱼体形态学及分子手段(Chen *et al*, 2016、2020; 陈生熬, 2019; 王锦秀等, 2021; 王新月等, 2022)。基于耳石是稳定硬组织的特点及其良好的信息储存功能，耳石不仅作为普遍的鱼龄鉴定材料，近年来国内外学者还将其广泛地应用于鱼类物种鉴别、种群结构、微化学生境履历分析和生活史策略等(Mesa *et al*, 2020; 谭博真等, 2020; Battaglia *et al*, 2010; 欧利国, 2020; 彭艳等, 2018; 王继隆等, 2019; 李孟孟等, 2017)。较鱼体形态学，耳石形态学具有易保存、操作重复性强、受环境影响小等优点，可作为其他组织的有效补充；较分子手段，基于耳石形态学开展群体鉴别成本更低、更便捷。故本研究将耳石形态学引入叶尔羌高原鳅的群体鉴

* 国家自然科学基金项目(31360635)、农业农村部财政专项(西北地区重点水域渔业资源与环境调查)、兵团科技局项目(2017DB003)和华中农业大学–塔里木大学联合基金(HNLH202006)共同资助。王新月，E-mail: 1072247070@qq.com
① 通信作者：陈生熬，教授，E-mail: chenshengao@163.com
收稿日期: 2022-02-28, 收修改稿日期: 2022-04-18

别，为其微化学分析和生活史策略的研究打下基础。

本研究以探究叶尔羌高原鳅耳石特征，比对耳石形态学对其不同地理群体鉴别的有效性为出发点，拟合耳石形态与体长和体质量的关系，为叶尔羌高原鳅的生长繁殖及资源管理提供理论支持，为进一步研究其种群组成和洄游生长提供参考；通过鱼体形态学、耳石形态测量法、椭圆傅里叶分析法比较不同河流叶尔羌高原鳅的种内差异，为传统形态分类提供有效补充，为高原渔业种质资源保护提供科学依据。

1 材料与方法

1.1 样品采集

2019—2021 年秋季在叶尔羌河(Yarkand River，Y)、和田河(Hotan River，H)和塔里木河(Tarim River，T)，用地笼(网目 2a=2.00 cm)随机采集叶尔羌高原鳅样本 734 尾(表 1)，现场进行生物学测定(殷名称, 1995)并解剖取出耳石，其他组织用 10%甲醛溶液固定，带回实验室进行后续处理。

表 1 叶尔羌高原鳅样本信息

Tab.1 Sample information of *T. yarkandensis*

群体 Population	采样时间 Sampling time	采样点 Sampling site	样本量 Sample number	体长 Body length/mm		体质量 Body weight/g	
				范围 Range	平均值±标准差 Mean±SD	范围 Range	平均值±标准差 Mean±SD
叶尔羌河 Yarkand River	2019.10	E 29°90′ N 38°00′	120	51.15~133.92	73.42±17.97	2.49~34.03	7.11±6.09
和田河 Hotan River	2020.10	E 80°80′ N 38°32′	321	43.34~137.34	90.41±13.49	1.09~35.11	11.06±4.84
塔里木河 Tarim River	2021.10	E 81°88′ N 40°80′	313	48.84~93.70	70.91±8.61	1.23~12.57	5.58±2.20

1.2 方法

1.2.1 鱼体形态学　传统形态学数据包括体质量(body weight)、全长(total length)、体长(body length)、体高(body height)、体宽(body width)、头长(head length)、吻长(snout length)、眼径(eye diameter)、眼间距(eye interval)、尾柄长(caudal peduncle length)和尾柄高(height of caudal peduncle)。框架法坐标点选择及框架数据指标选择见图 1。

采用数显游标卡尺(CD67-S15PS)测量长度(精度为 0.01 mm)，电子天平(LE403E)称量体质量(精度为 0.01 g)。

1.2.2 耳石形态学　使用体式显微镜(SMZ1270i)和 NIS Element 软件对叶尔羌高原鳅微耳石(图 2)进行拍照及形态指标测量，得到 6 个形态指标：耳石周长(otolith perimeter, OP)、耳石面积(otolith area, OA)、耳石长(otolith length, OL)、耳石宽(otolith width, OW)、耳石最大半径(maximum radius of otolith, R_{max})、耳石最小半径(minimum radius of otolith, R_{min})。

1.2.3 傅里叶分析法　椭圆傅里叶分析(Elliptic Fourier Descriptors, EFDs)，经灰阶转换、二值化图像

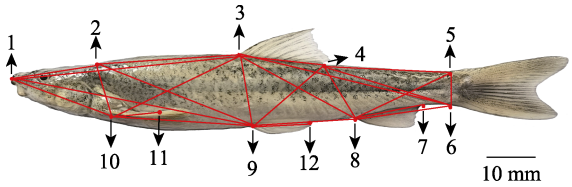

图 1 叶尔羌高原鳅的框架测量

Fig.1 Frame measurement of *T. yarkandensis*

1：吻端；2：枕后；3：背鳍起点；4：背鳍后基；5：尾鳍背部起点；6：尾鳍腹部起点；7：臀鳍后基；8：臀鳍起点；9：腹鳍起点；10：胸鳍起点；11：胸鳍后基；12：腹鳍后基。两坐标点间距离构成 24 项框架指标：1–2、2–3、3–4、4–5、5–6、6–8、8–9、9–10、10–1、1–9、2–10、2–9、3–1、3–10、3–9、3–8、3–6、4–9、4–8、4–6、5–8、10–11、9–12、8–7。

1: Tip of snout; 2: The last end of the frontal maxilla; 3: Origin of dorsal fin; 4: Terminus of dorsal fin; 5: Dorsal origin of caudal fin; 6: Ventral origin of caudal fin; 7: Terminus of anal fin; 8: Origin of anal fin; 9: Insertion of pelvic fin; 10: Insertion of pectoral fin; 11: Terminus of pectoral fin; 12: Terminus of pelvic fin. Twenty-four truss parameters are constructed by distance measurements between two coordinate points: 1–2, 2–3, 3–4, 4–5, 5–6, 6–8, 8–9, 9–10, 10–1, 1–9, 2–10, 2–9, 3–1, 3–10, 3–9, 3–8, 3–6, 4–9, 4–8, 4–6, 5–8, 10–11, 9–12, 8–7.

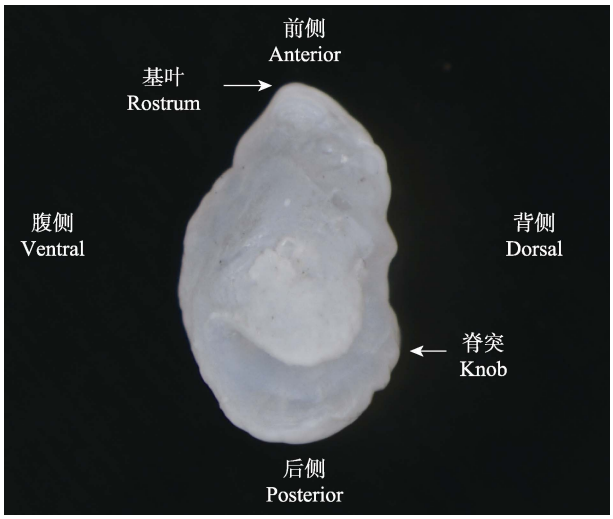

图 2　叶尔羌高原鳅左耳石外侧面示意图

Fig.2　View of external surface of the left lapillus otoliths of *T. yarkandensis* illustrating various features

处理、消除噪音、提取链码，每个耳石轮廓生成 20 个傅里叶谐波，每个谐波由 4 个系数(a、b、c、d)组成，共得到 80 个 EFDs 系数。因标准化时 a1 固定为 1，b1 和 c1 无限趋近于 0，故每个耳石整体形态轮廓信息一般由 77 个 EFDs 系数表达(欧利国等, 2019)。

1.3　数据处理

1.3.1　*鱼体形态指标*　　为消除样本规格差异对鱼体形态学指标的影响，每尾样本的所有实测长度数据采用头部特征除以头长、其他特征除以体长的方法予以校正，得到除体质量和体长外的 31 项比例性状。数据处理采用 Excel 软件。

1.3.2　*耳石形态特征*　　采用 Shapiro-Wilk 检验，基于偏度(Sk)、峰度(Ku)数值对耳石形态各指标进行正态性检验；参照谢桢桢等(2019)的方法，将 6 个耳石形态指标转化为 6 个形态因子和 7 个形态指数，见表 2。数据处理采用 NIS Element、SPSS18.0 软件。

1.3.3　*耳石形态与体长、体质量的关系*　　通过线性模型、幂函数模型、多项式模型、指数回归模型及对数模型拟合耳石主要形态指标与叶尔羌高原鳅体长、体质量的关系，依据 AIC (Akaike information criterion)准则选取最适模型，计算公式如下(Burnham *et al*, 2002)：

$$AIC=n\times\ln(RSS/n)+2k$$

式中，n 为样本数量；k 为方程中参数常数的数量；RSS 为残差平方和。数据处理采用 NIS Element、SPSS18.0、Origin9.0 软件。

1.3.4　*群体判别*　　采用逐步判别分析法，提取形态差异作用最显著的多项参数建立判别公式，计算判别准确率。数据处理采用 NIS Element、SPSS18.0 和 Shape 软件。

表 2　叶尔羌高原鳅耳石的形态因子与形态指标

Tab.2　Shape factors and morphological indices for otoliths of *T. yarkandensis*

形态因子 Shape factor	形态指标 Morphological index
$F1=OP/(OA)^{1/2}$	圆度 Roundness=$4OA/\Pi OL^2$
F2=OP/OL	形态因子 Format factor=$4\Pi OA/OP^2$
F3=OP/OW	环率 Circularity=OP^2/OA
$F4=(OA)^{1/2}/OL$	矩形趋近率 Rectangularity=OA/(OL×OW)
$F5=(OA)^{1/2}/OW$	椭圆率 Ellipticity=(OL+OW)/(OL–OW)
F6=OW/OL	半径比 Radius ratio=R_{max}/R_{min}
	幅形比 Aspect ratio=OL/OW

2　结果

2.1　耳石形态特征

叶尔羌高原鳅微耳石较小，近似椭圆形，中间较厚，逐渐向外边缘变薄，外侧面中央具明显突起。耳石长明显大于耳石宽，主间沟不明显，基叶发达，耳石腹部边缘较为光滑，呈浅弧形，耳石背部有波浪状突起。

配对样本 t 检验显示，叶尔羌高原鳅左右微耳石形态无显著差异($P>0.05$)，本研究中统一使用左耳石(表 3)。Shapiro-Wilk 检验表明，耳石面积(Sk=0.915, Ku=1.181)、耳石最小半径(Sk=0.499, Ku=0.153)、耳石最大半径(Sk=0.533, Ku=0.182)、耳石周长(Sk=0.517, Ku=0.288)、耳石长(Sk=0.562, Ku=0.209)和耳石宽(Sk=0.578, Ku=0.569)等各指标均不符合正态分布。

2.2　耳石形态与体长、体质量的关系

依据 AIC 值最小原则(表 4、表 5)，叶尔羌高原鳅耳石形态指标与体长、体质量的关系以对数函数为最佳拟合方程(图 3、图 4)建立回归方程(n=734)，进行相关性分析，R^2 范围在 0.48~0.62，相关性不高，拟合效果无显著差异($P>0.05$)，体长与叶尔羌高原鳅耳石形态指标相关性略高于体质量。

2.3　叶尔羌高原鳅不同群体判别比较

基于 Shape 软件提取叶尔羌高原鳅耳石外轮廓(图 5)，不同群体叶尔羌高原鳅存在耳石形态差异，进一步开展判别分析。由表 6 可知，常规的鱼体形态

表 3 叶尔羌高原鲅耳石形态参数值

Tab.3 Morphological parameters of otolith in *T. yarkandensis*

形态参数 Morphological parameter	叶尔羌河 Yarkand River		和田河 Hotan River		塔里木河 Tarim River	
	范围 Range	平均值±标准差 Mean±SD	范围 Range	平均值±标准差 Mean±SD	范围 Range	平均值±标准差 Mean±SD
耳石面积 OA/mm^2	0.39~1.54	0.87±0.18	0.29~1.06	0.56±0.14	0.24~0.84	0.53±0.14
耳石最小半径 R_{min}/mm	0.62~1.19	0.86±0.09	0.53~1.03	0.72±0.08	0.49~0.94	0.69±0.09
耳石最大半径 R_{max}/mm	0.85~1.75	1.33±0.15	0.71~1.49	1.03±0.15	0.66~1.32	1.01±0.14
耳石周长 OP/mm	2.36~4.84	3.58±0.41	1.97~3.91	2.86±0.38	1.88~5.17	2.86±0.48
耳石长 OL/mm	0.86~2.66	1.34±0.20	0.70~1.49	1.02±0.15	0.65~1.28	0.99±0.14
耳石宽 OW/mm	0.62~1.83	0.89±0.13	0.53~1.05	0.73±0.08	0.49~0.91	0.69±0.09

表 4 叶尔羌高原鲅耳石形态指标与体长关系拟合方程的 AIC 值比较

Tab.4 Comparison of morphological parameters of otolith with AIC values of different growth equations for body length

形态参数 Morphological parameter	线性方程 Linear	对数方程 Logarithmic	幂函数方程 Power	指数方程 Exponential
耳石面积 OA	–3 050.174 70	–3 052.386 64	–3 041.717 08	–321.129 24
耳石最小半径 R_{max}	–2 080.816 76	–3 749.732 48	–3 747.555 44	–442.776 39
耳石最大半径 R_{min}	–3 100.088 22	–3 120.882 21	–3 111.152 43	114.347 46
耳石周长 OP	–1 512.862 69	–1 533.823 43	–1 524.229 67	1 598.858 19
耳石长 OL	–2 937.542 39	–2 952.680 46	–2 945.122 56	105.191 67
耳石宽 OW	–3 524.074 73	–3 531.114 78	–3 529.892 82	–422.780 94

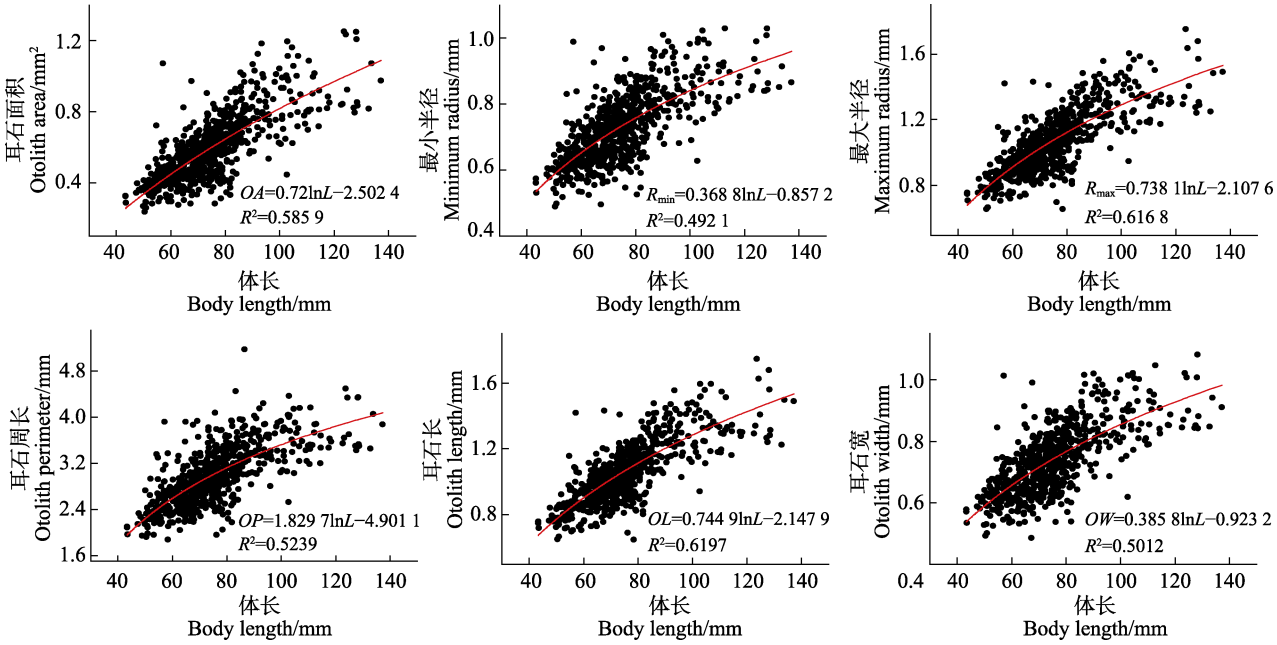

图 3 叶尔羌高原鲅耳石形态参数与体长的关系

Fig.3 Relationship between morphological parameters of otolith and body length of *T. yarkandensis*

学判别准确率均大于 90.0%，基于耳石形态的椭圆傅里叶分析法准确率均大于 80.0%，可作为叶尔羌高原鲅群体判别鉴定方法。

2.3.1 和田河群体与塔里木河群体比较 基于鱼体形态学方法对叶尔羌高原鲅和田河和塔里木河群体进行判别分析，筛选判别系数最大的参数即形态差异作用最显著，分别是头长、眼径、8–9、3–6、4–8、5–8、9–12、7–8，以 X_1~X_8 代替，建立判别式：

$$Y_H = -754.363 + 1\,083.724X_1 + 334.874X_2 + 279.518X_3 + 272.926X_4 + 267.890X_5 + 263.520X_6 - 253.284X_7 + 400.190X_8;$$

表 5　叶尔羌高原鲅耳石形态指标与体质量关系拟合方程的 AIC 值比较

Tab.5　Comparison of morphological parameters of otolith with AIC values of different growth equations for body weight

形态参数 Morphological parameter	线性方程 Linear	对数方程 Logarithmic	幂函数方程 Power	指数方程 Exponential
耳石面积 OA	–291.594 16	–3 024.812 57	–3 013.910 78	–684.761 13
耳石最小半径 R_{max}	–3 626.861 08	–3 736.881 90	–3 735.044 95	–442.776 39
耳石最大半径 R_{min}	–2 911.459 40	–3 072.187 51	–3 066.261 07	120.350 09
耳石周长 OP	–1 376.495 75	–1 507.315 32	–1 503.050 33	1 598.858 19
耳石长 OL	–2 776.462 59	–2 909.166 40	–2 904.399 40	111.191 48
耳石宽 OW	–3 424.907 80	–3 513.422 09	–3 512.379 29	–422.780 94

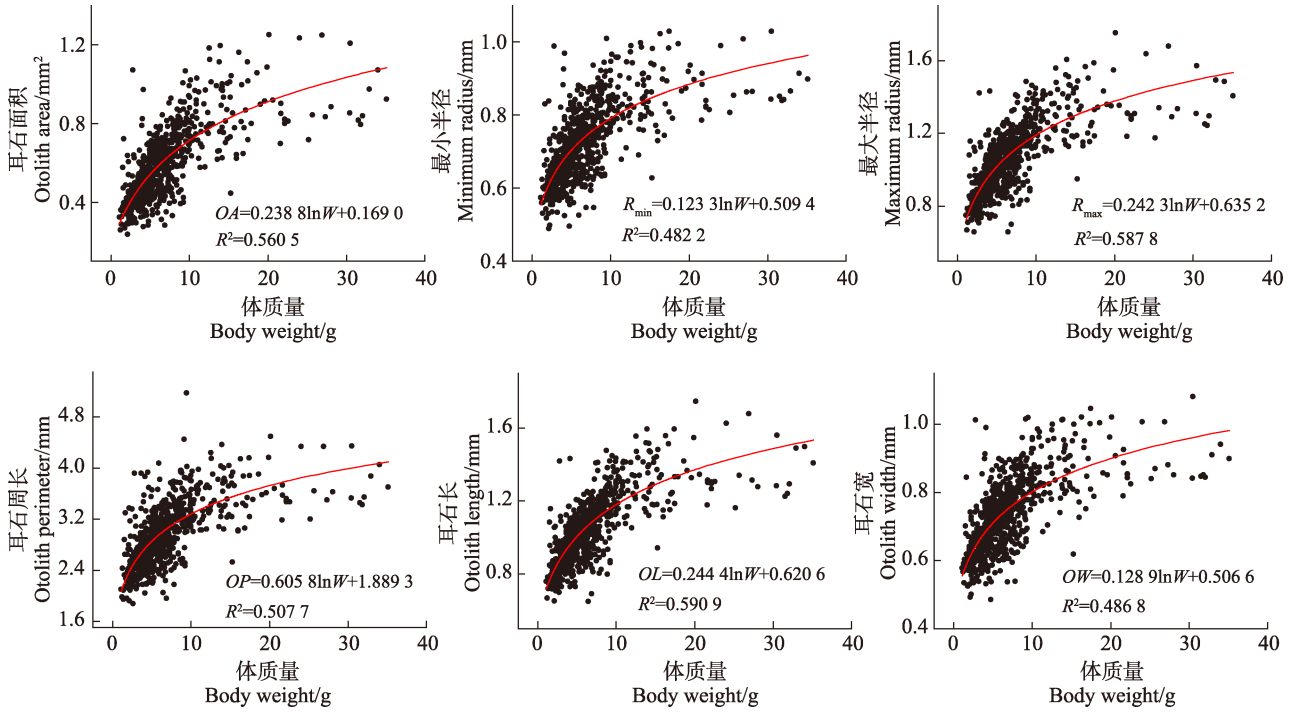

图 4　叶尔羌高原鲅耳石形态参数与体质量的关系

Fig.4　Relationship between morphological parameters of otolith and body weight of *T. yarkandensis*

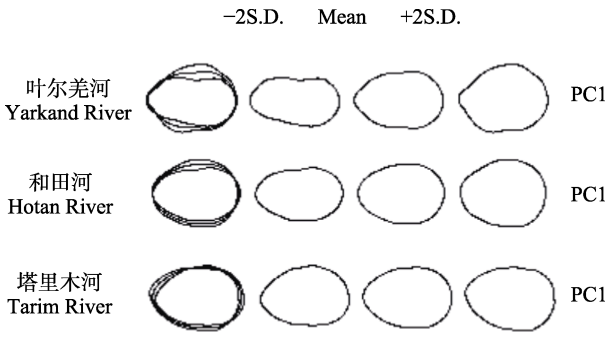

图 5　不同河流叶尔羌高原鲅耳石外轮廓

Fig.5　Outer contour of otolith for *T. yarkandensis* collected from different rivers

$$Y_T = -765.345+1\,080.053X_1+407.084X_2+315.256X_3+238.547X_4+238.434X_5+231.260X_6-449.899X_7+419.197X_8;$$

基于耳石形态测量法进行判别分析，筛选判别系数最大的参数是形态因子、圆度、幅形比、椭圆率、F2，以 X_1~X_5 代替，建立判别式：

$$Y_H = -44\,367.499+26\,121.376X_1-86\,564.057X_2+51\,480.547X_3-163\,355.968X_4+39\,357.468X_5;$$

$$Y_T = -44\,369.703+26\,136.450X_1-86\,612.301X_2+51\,471.603X_3-16\,3426.585X_4+39\,362.058X_5;$$

基于椭圆傅里叶分析法进行判别分析，筛选判别系数最大的参数是 a13、a16、a18、a19、a20、b14、b15、b17、b18、c15、c16、c18、d20，以 X_1~X_{14} 代替，建立判别式：

$$Y_H = -199.932+758.738X_1-2\,102.559X_2+726.672X_3-1\,107.394X_4-962.014X_5-754.826X_6-1\,177.008X_7-940.482X_8+2\,193.824X_9+1\,195.518X_{10}-918.204X_{11}-1\,850.064X_{12}-1\,107.443X_{13}+661.465X_{14};$$

表 6 叶尔羌高原鳅不同判别方法下的判别分析结果

Tab.6 Results of discriminant analysis for *T. yarkandensis* by different discriminant methods

群体 Population	判别方法 Discrimination method		
	鱼体形态 Fish body morphology	耳石形态测量法 Otolith morphology measurement	椭圆傅里叶分析法 Elliptic Fourier descriptors
和田河与塔里木河 Hotan River and Tarim River	96.0%	61.4%	82.2%
和田河与叶尔羌河 Hotan River and Yarkand River	93.0%	79.5%	87.9%
塔里木河与叶尔羌河 Tarim River and Yarkand River	96.5%	77.5%	86.8%

Y_T= –199.640+783.528X_1–1 951.237X_2+683.243X_3–1 138.197X_4–1 112.959X_5–700.998X_6–1 152.762X_7–894.934X_8+2 218.983X_9+1 291.767X_{10}–1 123.028X_{11}–1 973.454X_{12}–1 082.204X_{13}+724.591X_{14}。

2.3.2 叶尔羌河群体与和田河群体比较 基于鱼体形态学方法对叶尔羌高原鳅和田河和叶尔羌河群体进行判别分析，筛选判别系数最大的参数是体宽、眼径、2–3、8–9、10–1、1–9、4–9、4–6，以 X_1~X_8 代替，建立判别式：

Y_H= –668.713+389.423X_1+265.391X_2+486.391X_3+447.592X_4+396.093X_5+539.875X_6+570.868X_7+675.140X_8；

Y_Y= –681.434+288.918X_1+264.054X_2+538.090X_3+447.764X_4+370.297X_5+521.379X_6+587.450X_7+670.824X_8；

基于耳石形态测量法判别分析，筛选判别系数最大的参数是圆度、幅形比、椭圆率、F2、F3，以 X_1~X_5 代替，建立判别式：

Y_H= –55 356.713–22 149.057X_1+62 324.801X_2+42 712.676X_3+48 381.766X_4–27 766.797X_5；

Y_Y= –55 394.983–22 190.885X_1+62 387.283X_2+42 529.960X_3+48 393.094X_4–27 767.867X_5；

基于椭圆傅里叶分析法进行判别分析，筛选判别系数最大的参数是 a12、a13、b11、b12、b18、c14、c15、c16、d16、d18，以 X_1~X_{10} 代替，建立判别式：

Y_H= –416.030+4 455.567X_1+3 352.006X_2–3 978.189X_3–5 440.704X_4+6 959.784X_5–6 403.301X_6–3 937.816X_7–8 695.303X_8–4 967.260X_9–7 673.580X_{10}；

Y_Y= –400.877+4 455.259X_1+3 317.600X_2–3 809.155X_3–5 480.003X_4+6 839.061X_5–6 672.229X_6–4 243.988X_7–8 830.099X_8–4 917.392X_9–7 642.107X_{10}。

2.3.3 叶尔羌河群体与塔里木河群体比较 基于鱼体形态学方法对叶尔羌高原鳅叶尔羌河和塔里木河群体进行判别分析，筛选判别系数最大的参数是尾柄高、1–2、2–3、3–4、5–6、8–9、1–9、4–6，以 X_1~X_8 代替，建立判别式：

Y_Y= –459.682+602.652X_1+411.037X_2+358.023X_3+590.587X_4+304.627X_5+281.896X_6+223.528X_7+479.519X_8；

Y_T= –457.459+472.565X_1+358.121X_2+338.437X_3+536.212X_4+147.591X_5+320.927X_6+242.390X_7+467.632X_8；

基于耳石形态测量法进行判别分析，筛选判别系数最大的参数是形态因子、幅形比、椭圆率、F4，以 X_1~X_4 代替，建立判别式：

Y_Y= –36 264.928–21 268.574X_1+27 706.671X_2+50 957.276X_3+17 1304.008X_4；

Y_T= –36 120.795–21 251.167X_1+27 632.731X_2+50 969.229X_3+171 072.841X_4；

基于椭圆傅里叶分析法进行判别分析，筛选判别系数最大的参数是 a15、a16、a18、a19、a20、b14、b15、b16、b17、b18、b20、c15、c16、c18、d19，以 X_1~X_{15} 代替，建立判别式：

Y_Y= –189.680+1 031.189X_1–2 027.467X_2+1 212.271X_3–1 751.883X_4–960.044X_5–1 778.774X_6–1 038.040X_7–909.234X_8+2 547.771X_9+1 542.394X_{10}–1001.411X_{11}–1 284.393X_{12}–1 640.681X_{13}–1 034.732X_{14}–1 121.346X_{15}；

Y_T= –205.272+1 003.808X_1–1 942.790X_2+1 100.498X_3–1 975.260X_4–1 076.922X_5–1 794.153X_6–1 024.873X_7–1 089.052X_8+2 650.965X_9+1 671.729X_{10}–1 018.921X_{11}–1 405.119X_{12}–1 642.858X_{13}–1 014.032X_{14}–1 195.007X_{15}。

3 讨论

3.1 鱼类耳石形态与生长的相关性

水生动物生长发育过程中，不同生境下水体中矿物质元素在机体内的沉积有所不同，尤其体现在耳石等硬组织上，提取耳石形态特征不仅可以完成年龄识别，也是分类鉴别的有效手段(Sergio, 2007)。鱼类耳石形态的变化响应特定基因引导机制，也受水温、摄食行为、饵料丰度等因子影响(Ding *et al*, 2019; Morrison *et al*, 2019; Milošević *et al*, 2021)。耳石上元素的沉积决定耳石的形态和生长，随水域环境的变化，耳石生长与鱼类生长速度成线性相关(Souza *et al*, 2020)。叶尔羌高原鳅曾广泛分布于塔里木河水系，

栖息海拔较高、生境温度低，加之生存在高盐碱劣化水体等，在饵料生物极度贫瘠水域环境中，鱼体生长缓慢，耳石生长也较慢，这与 Souza 等(2020)和 Morrison 等(2019)等对河鲈(*Perca fluviatilis*)及花羔红点鲑(*Salvelinus malma*)开展耳石生长研究时得到的结论相似。本研究中，叶尔羌高原鳅唯冬季越冬时才进入深水区，其他季节喜沿边游动。Lombarte 等(2007)研究表明，随鱼类栖息水域深度变化，耳石大小随之呈正比变化，故栖息深度浅是造成叶尔羌高原鳅耳石规格过小的主要原因。

鱼类年龄鉴定中，可通过耳石半径来推算鱼类生长，表现出鱼体生长和耳石形态结构间的线性相关性(张涛等, 2017; 麻秋云等, 2013; 彭露等, 2018)。在统计分析中，R^2 可反映其相关性高低。本研究中的叶尔羌高原鳅耳石形态与体长、体质量的相关性 R^2<0.7。Battaglia 等(2010)和 Souza 等(2020)开展 16 种地中海深海鱼类和欧洲鲈鱼(*Perca fluviatilis*)体长、体质量与耳石形态关系的研究中 R^2>0.8。段咪等(2018)研究表明，在阿拉斯加狭鳕(*Gadus chalcogrammus*)的耳石形态与体长、体质量关系中 R^2 仅为 0.5，这与本研究中叶尔羌高原鳅耳石形态与体长、体质量较低的相关性相类似。Morrison 等(2019)研究指出，造成这种现象的原因是鱼类的洄游行为，鱼类洄游区域的变化继而引起摄食行为的变化，当洄游至优越的水体环境，获得更丰富营养饵料，机体快速生长，这与生物补偿性生长理论一致，即鱼类从完全或部分食物剥夺中再恢复时，其躯体倾向于加速生长(Fey, 2006; Mangel *et al*, 2005)。然而洄游区域停留时间较短，水体中矿物质元素无法在短期内实现快速沉积，机体生长加速不能完整呈现在耳石生长上，导致了耳石生长异速现象。陈生熬(2012)研究也指出，为集聚能量，叶尔羌高原鳅在洄游产卵前出现抢食行为，短期快速的补偿性生长影响了耳石和鱼体生长的相关性。以上研究都佐证了生境片段化条件下的短距离洄游行为是影响叶尔羌高原鳅耳石与鱼体生长相关性的主要原因。

3.2　耳石在鱼类群体鉴定分类中的应用

鱼类耳石形态具有高度物种特异性和群系特异性，不仅体现在不同物种间，同一物种不同生存环境下种群间及同一物种不同群体间也存在一定差异，这对鱼种识别及系统分类具有重要意义(王英俊, 2010)。Cerda 等(2021)评估了颈瘤鳚属(*Auchenionchus*) 2 种同域鱼类矢耳石形状，证实了矢耳石形态测量法在海洋鱼类鉴别中的有效性。Zhuang 等(2015)的研究也表明，基于耳石形态反映出的亲缘关系与其种内系统发育关系相吻合，为耳石与系统发育体系构建打下基础。

基于耳石形态开展鱼类群体划分，通过判别分析对不同种类的鉴别效果进行评价，结果也有所不同。宋超等(2020)研究发现，不同地理群体凤鲚(*Coilia mystus*)矢耳石形态指标存在显著差异(P<0.05)，判别准确率依次为温州群体(96.7%)、崇明群体(66.7%)、吕四群体(60.0%)和舟山群体(58.3%)。Zhuang 等(2015)基于耳石形态指标法和傅里叶分析法鉴别多群体鲽科(Pleuronectidae)判别准确率大于 95.00%。杨林林等(2020)研究发现，蓝点马鲛(*Scomberomorus niphonius*)海州湾和吕四渔场群体、象山湾和沙埕湾群体不存在显著差异(P>0.05)，渤海、黄海和东海群体间存在极显著差异(P<0.01)，综合判别率为 71.07%。本研究与上述分析方法一致，可对鉴别效果进行有效评估。不同群体叶尔羌高原鳅鱼体及耳石形态存在显著差异(P<0.05)，基于耳石形态测量法和椭圆傅里叶分析进行群体判别分析，和田河与塔里木河群体判别准确率分别为 61.4%和 82.2%，叶尔羌河与和田河群体分别为 79.5%和 87.9%，叶尔羌河与塔里木河群体分别为 77.5%和 86.8%，然而判别准确率不同，这与 **3.1** 涉及耳石生长异速现象的影响因素基本相同。

对比鱼体形态学，孙志成等(2020)通过 2 种方法判别斑尾刺虾虎鱼(*Acanthogobius ommaturus*)和黄鳍刺虾虎鱼(*A. flavimanus*)，准确率均为 100.0%，证明了不同判定方法的有效性，但在鱼体生长受限或机体损伤情况下，耳石形态可成为更有力的鉴别方法。本研究基于鱼体形态学判别叶尔羌高原鳅的准确率(>90.0%)略高于椭圆傅里叶分析法(>80.0%)，二者都可作为判别依据。叶尔羌高原鳅耳石规格过小是导致对总体样本开展耳石形态差异探究时判别准确率略低的重要原因，然而耳石形态学较传统鱼体形态学具有易保存、操作重复性强、受环境影响小等优点，尤其在肉食性鱼类内容物的食性分析、古脊椎动物探究等方面有着良好的应用前景(潘晓哲等, 2010)，故将耳石形态引入叶尔羌高原鳅的群体识别具有重要的研究价值。

耳石形态的种内差异受多因素影响，如宋超等(2020)研究发现，不同群体凤鲚间耳石形态差异大小与其洄游习性和地理阻隔程度密切相关，该短距离洄游性鱼类产卵主要选择在就近的近岸河口，地理位置相近群体耳石形态差异较小。结合叶尔羌高原鳅洄游习性和对塔里木河水系的调查，发现水利工程建设导致叶尔羌高原鳅原有生境破碎化，严重影响其生殖洄游行为，形成不同地理群体，这与上述研究结果相吻合，故耳石形态差异与鱼类行为和栖息环境有关。鉴于耳石在叶尔羌高原鳅群体分类判别中的有效性，可

进一步在高原鱼类鉴定分类中应用。

4 结论

叶尔羌高原鰁耳石形态与机体的生长相关性较强，以对数方程为最佳拟合关系，反映个体发育对水域环境的适应，而洄游行为则是影响其耳石形态与鱼体形态关系的主要原因。不同物种或同一物种不同地理群体鱼类耳石形态存在差异，是因为个体发生和环境因子共同作用，叶尔羌高原鰁耳石的变化与塔里木河水量减少、盐碱加剧及饵料缺乏等特殊生态环境密切相关。叶尔羌高原鰁不同地理群体多种方法判别比较中，基于鱼体形态学的各群体判别准确率均高于90.0%，基于耳石形态的椭圆傅里叶分析法的判别准确率均高于 80.0%，证实了耳石形态差异对群体划分的可行性。本研究为构建高原特有鱼类耳石系统分类检索体系积累数据，进一步夯实高原鰁属分类学数据库建设，为渔业资源动态评估和管理提供依据，推动水产种业可持续发展。

参 考 文 献

BATTAGLIA P, MALARA D, ROMEO T, *et al*. Relationships between otolith size and fish size in some mesopelagic and bathypelagic species from the Mediterranean Sea (Strait of Messina, Italy). Scientia Marina, 2010, 74(3): 605–612

BERMEJO S. Fish age classification based on length, weight, sex and otolith morphological features. Fisheries Research, 2007, 84(2): 270–274

BURNHAM K P, ANDERSON D R. Model selection and multi-model inference: A practical information–Theoretical approach. Springer, 2002

CERDA J M, PALACIOS-FUENTES P, DÍAZ-SANTANA-ITURRIOS M, *et al*. Description and discrimination of sagittae otoliths of two sympatric labrisomid blennies *Auchenionchus crinitus* and *Auchenionchus microcirrhis* using morphometric analyses. Journal of Sea Research, 2021, 173: 102063

CHEN S A, HOU J L, YAO N, *et al*. Comparative transcriptome analysis of *Triplophysa yarkandensis* in response to salinity and alkalinity stress. Comparative Biochemistry and Physiology Part D: Genomics and Proteomics, 2020, 33: 100629

CHEN S A, YAO N, XIE C X, *et al*. Complete mitochondrial genome of the *Triplophysa* (*Hedinichthys*) *yarkandensis* (Day). Mitochondrial DNA Part B: Resources, 2016, 1(1): 235–236

CHEN S A. Early development and physiological mechanism of salinity-alkalinity adaption of *Triplophysa yarkandensis* (Day). Doctoral Dissertation of Huazhong Agricultural University, 2019 [陈生熬. 叶尔羌高原鰁早期发育及盐碱适应生理机制. 华中农业大学博士研究生学位论文, 2019]

CHEN S A. Study on population ecology of *Triplophysa yarkandensis* (Day) in Tarim River. Master′s Thesis of Huazhong Agricultural University, 2012 [陈生熬. 塔里木河叶尔羌高原鰁种群生态学研究. 华中农业大学硕士研究生学位论文, 2012]

DING L Y, TAO J, DING C Z, *et al*. Hydrogeomorphic factors drive differences in otolith morphology in fish from the Nu-Salween River. Ecology of Freshwater Fish, 2019, 28(1): 132–140

DUAN M, WEI L, ZHU G P. Morphometric features of sagittal otolith for Alaska pollock *Gadus chalcogrammus* in the western Bering Sea. Journal of Dalian Ocean University, 2018, 33(4): 492–498 [段咪, 魏联, 朱国平. 西白令海阿拉斯加狭鳕矢耳石形态特征研究. 大连海洋大学学报, 2018, 33(4): 492–498]

FEY D P. The effect of temperature and somatic growth on otolith growth: The discrepancy between two clupeid species from a similar environment. Journal of Fish Biology, 2006, 69(3): 794–806

GUO Y, ZHANG R M, CAI L G. Fishes of Xinjiang. Urumqi: Xinjiang Science and Technology Press, 2012 [郭焱, 张人铭, 蔡林刚. 新疆鱼类志. 乌鲁木齐: 新疆科学技术出版社, 2012]

LI M M, JIANG T, KHUMBANYIWA D D, *et al*. Reconstructing habitat history of *Coilia nasus* from the Hexian section of the Yangtze River in Anhui Province by otolith microchemistry. Acta Hydrobiologica Sinica, 2017, 41(5): 1054–1061 [李孟孟, 姜涛, KHUMBANYIWA Davison Daniel, 等. 基于耳石微化学的长江安徽和县江段刀鲚生境履历重建. 水生生物学报, 2017, 41(5): 1054–1061]

LOMBARTE L A, CRUZ A. Otolith size trends in marine fish communities from different depth strata. Journal of Fish Biology, 2007, 71(1): 53–76

MA Q Y, XUE Y, XU B D, *et al*. Relationships between otolith size and fish size for twelve prey fish species from Jiaozhou Bay. Acta Hydrobiologica Sinica, 2013, 37(3): 481–487 [麻秋云, 薛莹, 徐宾铎, 等. 胶州湾 12 种饵料鱼类耳石大小与体长的关系. 水生生物学报, 2013, 37(3): 481–487]

MANGEL M, MUNCH S B. A life-history perspective on short-and long-term consequences of compensatory growth. American Naturalist, 2005, 166(6): E155–E176

MESA M L, GUICCIARDI S, DONATO F, *et al*. Comparative analysis of otolith morphology in icefishes (Channichthyidae) applying different statistical classification methods. Fisheries Research, 2020, 230: 105668

MILOŠEVIĆ D, BIGOVIĆ M, MRDAK D, *et al*. Otolith morphology and microchemistry fingerprints of European eel, *Anguilla anguilla* (Linnaeus, 1758) stocks from the Adriatic Basin in Croatia and Montenegro. Science of the Total Environment, 2021, 786(1): 147478

MORRISON C M, KUNEGEL-LION M, GALLAGHER C P, *et al*. Decoupling of otolith and somatic growth during anadromous migration in a northern salmonid. Canadian Journal of Fisheries and Aquatic Sciences, 2019, 76(11): 1940–1953

OU L G, LIU B L, FANG Z. Identification of sagittal otolith morphology and sulcus morphology based on elliptic Fourier transform. Marine Fisheries, 2019, 41(4): 385–396 [欧利国, 刘必林, 方舟. 基于椭圆傅里叶变换的鱼类矢耳石和听沟形态识别. 海洋渔业, 2019, 41(4): 385–396]

OU L G. Identification of Carangidae species in Dongsha Islands of the South China Sea based on otolith morphological information. Master´s Thesis of Shanghai Ocean University, 2020 [欧利国. 基于耳石形态信息的南海东沙海域鲹科鱼类识别. 上海海洋大学硕士研究生学位论文, 2020]

PAN X Z, GAO T X. Sagittal otolith shape used in the discrimination of fishes of the genus *Sillago* in China. Acta Zootaxonomica Sinica, 2010, 35(4): 799–805 [潘晓哲, 高天翔. 基于耳石形态的鳍属鱼类鉴别. 动物分类学报, 2010, 35(4): 799–805]

PENG L, JIANG Y E, XU S N, *et al*. Otolith morphology of *Nemipterus virgatus* and its relation to body length and mass in continental shelf of northern South China Sea. South China Fisheries Science, 2018, 14(6): 27–33 [彭露, 江艳娥, 徐姗楠, 等. 南海北部陆架区金线鱼矢耳石形态及其与体长、体质量关系. 南方水产科学, 2018, 14(6): 27–33]

PENG Y, ZENG Y, ZHANG C, *et al*. Otolith morphology of *Saurogobio dabryi* and the variance in different sections of Jialing River. Journal of Fisheries of China, 2018, 42(12): 1896–1905 [彭艳, 曾燏, 张臣, 等. 嘉陵江不同江段蛇鮈耳石形态特征及差异. 水产学报, 2018, 42(12): 1896–1905]

SONG C, YANG Q, ZHAO F, *et al*. Otolith morphological variations among four geographic populations of *Coilia mystus* in the Yangtze estuary and its adjacent waters. Journal of Fishery Sciences of China, 2020, 27(10): 1125–1135 [宋超, 杨琴, 赵峰, 等. 长江口及邻近海域 4 个不同地理群体凤鲚矢耳石形态差异. 中国水产科学, 2020, 27(10): 1125–1135]

SOUZA A T, SOUKALOVÁ K, DĚD V, *et al*. Ontogenetic and interpopulation differences in otolith shape of the European perch (*Perca fluviatilis*). Fisheries Research, 2020, 230: 105673

SUN Z C, LI Y D, SONG C Y, *et al*. Comparative studies on morphology and genetics between *Acanthogobius ommaturus* and *Acanthogobius flavimanus*. Journal of Fisheries of China, 2020, 44(8): 1237–1248 [孙志成, 李亚东, 宋晨雨, 等. 斑尾刺虾虎鱼和黄鳍刺虾虎鱼的形态学、遗传学比较. 水产学报, 2020, 44(8): 1237–1248]

TAN B Z, YANG X F, YANG R B. Age structure and growth characteristics of *Gymnocypris waddelli* in the Zhegu Lake, Tibet. Journal of Fishery Sciences of China, 2020, 27(8): 879–885 [谭博真, 杨学芬, 杨瑞斌. 西藏哲古错高原裸鲤年龄结构与生长特性. 中国水产科学, 2020, 27(8): 879–885]

WANG J L, LIU W, WANG C, *et al*. Microchemistry analysis of otoliths of *Coregonus ussuriens*is from the Heilong River Basin. Acta Hydrobiologica Sinica, 2019, 43(4): 825–831 [王继隆, 刘伟, 王臣, 等. 基于耳石微化学的乌苏里白鲑生境履历分析. 水生生物学报, 2019, 43(4): 825–831]

WANG J X, REN D Q, WANG X Y, *et al*. The analysis of genetic diversity of *Triplophysa yarkandensis* (Day) from five geographic populations in the Tarim River Basin. Progress in Fishery Sciences, 2021, 42(4): 46–54 [王锦秀, 任道全, 王新月, 等. 塔里木河流域 5 个地理种群的叶尔羌高原鳅遗传多样性分析. 渔业科学进展, 2021, 42(4): 46–54]

WANG X Y, ZHANG Y J, LIU F, *et al*. Analysis on the morphological differences of *Triplophysa yarkandensis* in different geographic populations. Progress in Fishery Sciences, 2022, 43(6): 199–206 [王新月, 张永杰, 刘斐, 等. 叶尔羌高原鳅不同地理群体形态差异分析. 渔业科学进展, 2022, 43(6): 199–206]

WANG Y J. The application of Fourier analysis in the research of otolith morphology. Master´s Thesis of Ocean University of China, 2010 [王英俊. 傅里叶分析在鱼类耳石形态学中的应用研究. 中国海洋大学硕士研究生学位论文, 2010]

XIE Z Z, ZHANG H H, HU L X, *et al*. Comparative studies on multivariate morphometrics of asteriscus of four culters. Journal of Huazhong Agricultural University, 2019, 38(1): 82–90 [谢桢桢, 张化浩, 胡良雄, 等. 4 种鲌的星耳石形态度量学比较. 华中农业大学学报, 2019, 38(1): 82–90]

YANG L L, JIANG Y Z, LIU Z L, *et al*. Morphological comparison in the sagittal otolith of spawning population of *Scomberomorus niphonius* in coastal water of China. Marine Fisheries, 2020, 42(3): 287–295 [杨林林, 姜亚洲, 刘尊雷, 等. 中国沿海蓝点马蛟繁殖群体的耳石形态差异. 海洋渔业, 2020, 42(3): 287–295]

YIN M C. Fish ecology. Beijing: China Agriculture Press, 1995 [殷名称. 鱼类生态学. 北京: 中国农业出版社, 1995]

ZHANG T, WANG H H, BI X J, *et al*. Sagittal otolith growth and development at different development stages in larval and juvenile *Coilia mystus* in the Yangtze estuary. Journal of Fishery Sciences of China, 2017, 24(6): 1315–1322 [张涛, 王焕焕, 毕学娟, 等. 长江口凤鲚仔稚鱼不同发育阶段矢耳石生长. 中国水产科学, 2017, 24(6): 1315–1322]

ZHUANG L C, YE Z J, ZHANG C. Application of otolith shape analysis to species separation in *Sebastes* spp. from the Bohai Sea and the Yellow Sea, northwest Pacific. Environmental Biology of Fishes, 2015, 98(2): 547–558

(编辑　马璀艳)

Otolith Morphology and Population Discrimination of *Triplophysa yarkandensis*

WANG Xinyue[1], CHEN Sheng´ao[1,2①], WANG Chengxin[1], ZI Fangze[1],
CHANG Desheng[1], XU Hao[1], LI Dapeng[2]

(1. *College of Life Sciences and Technology, Tarim University, Tarim Research Center of Rare Fishes, Alar* 843300, *China*;
2. *College of Fisheries, Huazhong Agricultural University, Wuhan* 430070, *China*)

Abstract To study the classification, identification, and discrimination between different geographical populations of *Triplophysa yarkandensis* and explore the related otolith morphology and fish life history, this study statistically analyzed the morphological otolith indices and fish bodies of 734 *T. yarkandensis* from the Yarkand River, Hotan River, and Tarim River using otolith morphology and fish ecology methods. The results showed that otoliths were small in *T. yarkandensis*, approximately elliptic, thicker in the middle, gradually thinning to the outer edge, and with a prominent protrusion in the center of the external surface. Otolith length was obviously larger than otolith width while the excisural notch was not obvious, wherein the rostrum was developed, the ventral otolith edge was smooth with a shallow arc, and the otolith dorsal had a crest-like ridge. No significant difference between left and right lapillus morphology was observed (P>0.05). The otolith morphological indices followed a logarithmic function with the body length and weight (R^2=0.48~0.62). It reflects the ontogenetic adaptation to the environment, and migration behavior mainly affects the relationship between otolith morphology and fish body morphology. The SHAPE software was used to extract the outer otolith contour of *T. yarkandensis*, revealing morphological differences between *T. yarkandensis* populations. The parameter with the largest discriminant coefficient, *i.e.*, the one in which the morphological difference has the greatest significant effect, was screened. Therewith, the discriminant formula was set up to calculate the discriminant accuracy. Discriminant analysis between groups using fish morphology, otolith morphometry and elliptical Fourier analysis, respectively. The discriminant accuracy of the Hotan River and Tarim River populations was 96.0%, 61.4%, and 82.2%; the Yarkand River and Hotan River was 93.0%, 79.5%, and 87.9%; the Yarkand River and Tarim River populations was 96.5%, 77.5%, and 86.8%. Environmental factors such as water temperature, spatial niche adaptation, and habitat depth were the main causes of the otolith morphological changes, also affecting the behavior characteristics of typical *T. yarkandensis* life history, especially fish migration. In this study, the *T. yarkandensis* was found to live in high altitude, low habitat temperature, and high salinity and alkaline waters, so the fish body growth and the elements deposition rate onto otoliths were low. *T. yarkandensis* belongs to the sub-cold water and benthic fish group, which only enters deep water during overwintering in winter. In other seasons, it swims along the edge and rests in shallow depth waters, so the otolith grows slowly and has a small size. The relationship between otolith and body growth reflected the *T. yarkandensis* ontogenetic adaptability to its habitat. As the *T. yarkandensis* residence time is short in the migration area, mineral elements in the water body cannot be rapidly deposited in a short period of time, and the accelerated body growth is not completely reflected in the otolith growth. Therefore, the short-distance migration behavior under habitat fragmentation mainly affects the correlation between otolith and fish growth in *T. yarkandensis*. The fish otolith morphology is highly species-specific and population-specific. *T. yarkandensis* otolith morphology

① Corresponding author: CHEN Sheng´ao, E-mail: chenshengao@163.com

was significantly different among the geographically different populations (P<0.05). In this study, the accuracy rate (>90.0%) was slightly higher than that of elliptic Fourier analysis (>80.0%), both of which could be used as the discrimination basis parameter. However, the traditional fish otolith morphology is easy to record, as repetitive operations are robust and less affected by the environment, especially in the contents of a carnivorous fish feeding analysis; therefore, vertebrate paleontology explore has a useful application prospect in these aspects. Moreover, it could serve as an effective tool to identify fish intraspecific differences in the case of growth restriction or bodily injury. Therefore, it is of great research value to introduce the otolith morphology into the population identification of *T. yarkandensis*. This study explored the *T. yarkandensis* morphological characteristics and compared otolith morphologies to effectively identify the geographically different population, co-relating otolith shape with *T. yarkandensis* growth (*i.e.*, body length and quality) and resource management, providing theoretical support to further researches about the composition and migratory population growth. The *T. yarkandensis* intraspecies differences in different rivers were also compared concerning fish body morphology, otolith measurements, and elliptic Fourier analysis, providing strong evidence for traditional morphological classification. The effective utilization and cost control of incomplete fish samples was greatly favored by this study. Otolith morphology was applied for the first time in the classification and population identification of *T. yarkandensis*, which laid a foundation for the development and research of its microchemical features and life history strategy, presenting a reference for further identification and evolutionary classification of *Triplophysa*, strengthening the taxonomic foundation of aquatilia, and providing scientific basis for protecting the plateau fishery germplasm resources.

Key words *Triplophysa yarkandensis*; Otolith; Morphological difference; Discriminant analysis